

Kinetic study of hydrogen peroxide decomposition by catalase in a flow-mix microcalorimetric system

Marcello Fidaleo^a, Roberto Lavecchia^{b,*}

^a *Istituto di Tecnologie Agroalimentari, Università della Tuscia, Via S. Camillo de Lellis I-01100 Viterbo, Italy*

^b *Dipartimento di Ingegneria Chimica, Università "La Sapienza", Via Eudossiana 18 I-00184 Roma, Italy*

Received 4 September 2002; accepted 14 October 2002

Abstract

The kinetics of hydrogen peroxide decomposition by the enzyme catalase was studied at pH 7.4 in the temperature range 10–30 °C. Experiments were performed by the LKB-2277 Thermal Activity Monitor equipped with a flow-mix cylinder. The calorimetric reaction unit was schematised as a tubular reactor operating under plug-flow conditions. A first-order kinetic expression, with respect to both the substrate and the enzyme, was used to describe the rate of hydrogen peroxide decomposition. Regression analysis of calorimetric data provided a molar reaction enthalpy of $-87.55 \text{ kJ mol}^{-1}$ and an activation energy of 11 kJ mol^{-1} . Analysis of model residuals and the normal probability plot indicated that the results obtained were statistically significant.

© 2002 Elsevier Science B.V. All rights reserved.

Keywords: Catalase; Hydrogen peroxide; Enzyme kinetics; Microcalorimeter

1. Introduction

Microcalorimetry is a powerful tool for investigating physical or chemical transformations accompanied by the evolution or absorption of heat. The high accuracy and simplicity of this technique, along with its insensitivity to the optical or electrochemical properties of the sample, make it extremely versatile [1–3]. Measurement of heat effects can be carried out in batch mode, or with continuous or interrupted flow methods. Selecting the appropriate mode of operation depends on the properties of the sample and the nature of the phenomena to be investigated.

In flow-mix systems two liquid streams are fed separately to the instrument. After thermal equilibration, the liquids are efficiently mixed and the resulting mixture flows through a detecting tube, where heat effects are monitored. Flow-mix operations can be used for a variety of aims in such different fields as thermodynamics, material science and chemical kinetics. An examination of the literature reveals that most applications have been concerned with the determination of the heat of mixing or other thermodynamic properties of liquid solutions [4–7]. Further thermodynamic research has been focused on characterising ligand–protein interactions [8], studying the formation of inclusion complexes [9], and analysing the transfer of solutes between two immiscible phases [10]. By contrast, only a few studies have been published on the use of flow-mix calorimetry for kinetic investigations [11–13]. This is rather surprising, since this tech-

* Corresponding author. Tel.: +39-6-44585451;

fax: +39-6-4827453.

E-mail address: roberto.lavecchia@uniroma1.it (R. Lavecchia).

Nomenclature

<i>A</i>	reactor cross-sectional area (m ²)
<i>e</i>	enzyme concentration (kg m ⁻³)
<i>E_a</i>	activation energy (J mol ⁻¹)
<i>F</i>	standard normal distribution function
<i>G</i>	free energy (J mol ⁻¹)
<i>H</i>	enthalpy (J mol ⁻¹)
<i>k</i>	rate constant (m ³ kg ⁻¹ s ⁻¹)
<i>N</i>	number of data
<i>P</i>	number of parameters
<i>Q</i>	thermal power (W)
<i>r_s</i>	reaction rate (mol s ⁻¹ m ⁻³)
<i>R</i>	model residual (W)
<i>R</i>	universal gas constant (J mol ⁻¹ K ⁻¹)
<i>s</i>	substrate concentration (mol m ⁻³)
<i>T</i>	temperature (K)
<i>T[*]</i>	kinetic parameter (K)
<i>v</i>	liquid flow rate (m ³ s ⁻¹)
<i>V</i>	reactor volume (m ³)
<i>X</i>	substrate conversion
<i>Y</i>	normal-order statistics median
<i>z</i>	axial co-ordinate (m)

Greek letters

Φ	objective function (W ²)
τ_c	mean residence time (s)
τ_r	characteristic reaction time (s)

Subscripts

<i>j</i>	generic point
out	outlet
0	inlet
∞	steady-state value

Superscripts

*	normalised
calc	calculated
exp	experimental

nique is potentially most productive. Thermal-power signal magnitudes can be directly related to reaction rates, so that knowledge can be acquired on the behaviour of the reacting system in a continuous-flow reactor. In addition, both thermodynamic and kinetic parameters can be determined from analysis of these data.

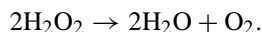
In this paper, we report the results of a microcalorimetric study on the kinetics of hydrogen peroxide decomposition by the enzyme catalase. There is much interest on this enzyme, from both a fundamental and a practical viewpoint. Catalase is found in nearly all aerobic micro-organisms, animals and plants, where it protects cells against oxidative damage from hydrogen peroxide [14]. The enzyme is also of interest in the field of enzyme biosensors [15,16] and wherever hydrogen peroxide is used for sterilisation/disinfection purposes [17].

Our specific interest in catalase arose within the research we are carrying out on a new generation of extracorporeal membrane oxygenators in which catalase is used to produce oxygen by decomposition of hydrogen peroxide [18]. The analysis and design of such devices require the availability of accurate kinetic data for the catalase reaction at the average blood pH, 7.4, and at the relatively low substrate and enzyme concentrations needed for their operation. To get this kind of information we used an isothermal microcalorimeter equipped with a flow-mix measuring cylinder.

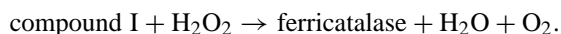
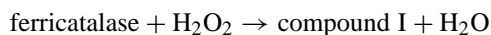
2. The catalase–hydrogen peroxide system

Catalase exhibits a high degree of structural complexity [19]. The enzyme molecules are oligomers composed of four tetrahedrally-arranged 60,000 Da subunits. Each subunit consists of a single polypeptide chain and is associated with a ferric protoporphyrin IX as prosthetic group. The resulting tetramer is relatively stable, although the association of subunits has been found to rely only on noncovalent, mainly hydrophobic, interactions.

The overall enzyme-catalysed reaction can be represented as



The mechanism by which the reaction proceeds is believed to involve the cycling of catalase between its ferric ground state (ferricatalase) and a two-electron-oxidised state (compound I) [20]:



As regards the reaction kinetics, two major considerations deserve attention [20,21]:

- (i) saturation of catalase by H_2O_2 does not occur until a substrate concentration of about 5 M;
- (ii) at H_2O_2 concentrations above 0.1 M the enzyme is rapidly inactivated by the substrate.

It then follows that estimation of the intrinsic kinetic parameters of reaction should be accomplished by performing experiments at sufficiently low substrate concentrations ($\ll 0.1$ M). Under these conditions the kinetics of hydrogen peroxide decomposition can be considered of first-order with respect to the substrate [20].

The enzyme kinetics is also known to have a very small temperature dependence, due to the low energy of activation. Above 30°C a decrease in activity has been observed indicating incipient thermal inactivation [22].

3. Experimental

3.1. Materials

Catalase (EC 1.11.1.6) from bovine liver was obtained from Sigma (USA) as a lyophilised and chromatographically purified powder. The claimed activity was $21,000 \text{ U mg}^{-1}$, where 1 U corresponds to the amount of enzyme that decomposes $1 \mu\text{mol}$ of H_2O_2 per min at pH 7 and 25°C .

Hydrogen peroxide was purchased from Sigma, as a stabilised 30 wt.% solution in water, and was stored at 4°C . All other chemicals were of reagent grade and used without further purification.

Fresh substrate and enzyme solutions were prepared immediately before each experiment by dis-

solving the products in 0.1 M phosphate buffer ($\text{KH}_2\text{PO}_4 + \text{Na}_2\text{HPO}_4$) at pH 7.4.

3.2. Methods

The reaction kinetics was investigated by a four-channel isothermal microcalorimeter (LKB 2277 Thermal Activity Monitor) manufactured by ThermoMetric (Sweden). The system essentially consists of a thermostatic water bath of about 23 l, a high-precision control unit performing digital calibration and dynamic correction of output signal, and an external water circulator. This latter had a capacity of about 6 l and allowed temperature to be controlled within $\pm 0.02^\circ\text{C}$. The system was completed by a two-channel peristaltic pump. It was accurately calibrated by determining the volumes of bidistilled water pumped, in a given time, for assigned values of the step motor's rotary speed. According to the manufacturer, the microcalorimeter equipped with the external thermostat can operate between 5 and 90°C with a stability better than $\pm 0.0001^\circ\text{C}$ over 24 h.

In the water bath up to four measuring cylinders can be housed, each of which can operate on batch samples or under a variety of flow configurations. We used a flow-mix cylinder. In this unit the two liquid streams flow through two separate heat exchanger coils, where thermal equilibration at the bath temperature occurs. They enter into a high-efficiency mixing cell and the resulting mixture passes through a spiral of gold tubing, with an effective volume of about 0.65 cm^3 . This zone is in close contact with a pair of Peltier elements for detection of thermal effects. A schematic representation of the system and the mode of operation are shown in Fig. 1.

In a typical experiment, the thermostatic bath was conditioned at the desired temperature for a time

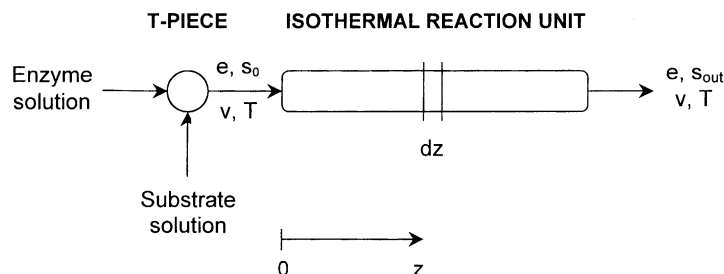


Fig. 1. Simplified outline of the flow-mix apparatus. The main operating parameters are also indicated.

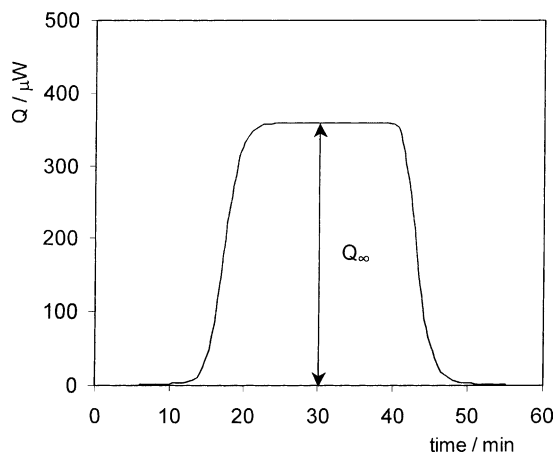


Fig. 2. Thermal power (Q) as a function of time in a flow-mix kinetic experiment. Q_{∞} is the steady-state value. The conditions of the run are: $T = 15^{\circ}\text{C}$, $e = 1.8 \times 10^{-4} \text{ g l}^{-1}$, $s_0 = 3 \text{ mM}$.

sufficient to reach equilibration. Then the enzyme solution was fed, at the selected flow rate, to both inlet tubings. Once a stable baseline was obtained, one of the tubing was removed from the enzyme-containing flask and inserted into the flask with the substrate solution. As the substrate and the enzyme began to mix, reaction started and the thermal-power signal progressively increased, until a steady-state value was reached. After a time sufficient to check the stability of the steady-state level the reaction was stopped by moving the substrate tubing back to the enzyme flask. The signal then declined to the baseline level. An example of a recorded calorimetric curve is displayed in Fig. 2.

In all experiments, the substrate and the enzyme solutions were fed at a flow rate of $0.115 \text{ cm}^3 \text{ min}^{-1}$, corresponding to an overall flow rate in the reaction unit of $0.23 \text{ cm}^3 \text{ min}^{-1}$. The explored temperature range was $10\text{--}30^{\circ}\text{C}$, the inlet substrate concentration was varied between 2 and 10 mM, and the inlet enzyme concentration between 1.8×10^{-4} and $6.8 \times 10^{-2} \text{ g l}^{-1}$.

To assess whether hydrogen peroxide could undergo a nonenzymatic decomposition, blank runs were made in which pure phosphate buffer and a 10 mM substrate solution were fed to the calorimeter. Similarly, in order to monitor eventual thermal effects related to the enzyme inactivation or conformational changes, mixing experiments were made using a highly concentrated catalase solution and the buffer alone. In both cases no appreciable signal was detected.

4. Results and discussion

To investigate the kinetics of hydrogen peroxide decomposition we performed seven sets of experiments, under the conditions summarised in Table 1. They were realised to estimate the heat of reaction (series A) and the kinetic parameters (series B–F). In the former experiments much higher enzyme concentrations were used, for the reason that will be discussed later. The run at the mean temperature, 20°C , was duplicated (series D and D bis) to measure the repeatability of the experimental procedure. The observed variations were within $\pm 2\%$.

4.1. Kinetic modelling of the flow-mix reaction zone

Due to its length to diameter ratio (>200) the reaction unit was schematised as a tubular plug-flow reactor.

To relate the measured steady-state thermal powers (Q_{∞}) to the temperature and substrate concentration we need to solve the mass-balance equation for the substrate, and the energy-balance equation.

Formulation of the mass-balance equation on a reactor element of length dz (see Fig. 1), under isothermal and steady-state conditions, leads to the following ordinary differential equation:

$$\frac{ds}{dz} + \frac{r_s A}{v} = 0 \quad (1)$$

where s is the substrate concentration at z and r_s the corresponding reaction rate. If a first-order kinetics, with respect to both the substrate and the enzyme, is assumed we have

$$r_s = k_e s \quad (2)$$

Table 1
Outline of the experimental conditions (e and s_0 are the enzyme and substrate concentrations at the inlet of the reaction unit)

Data set	T ($^{\circ}\text{C}$)	Number of data	e (g l^{-1})	s_0 (mM)
A	25	4	3.4×10^{-2} to 6.8×10^{-2}	4.9–6.2
B	10	7	1.8×10^{-4}	2–10
C	15	7	1.8×10^{-4}	2–10
D	20	8	1.8×10^{-4}	2–10
D bis	20	8	1.8×10^{-4}	2–10
E	25	7	1.8×10^{-4}	2–10
F	30	7	1.8×10^{-4}	2–10

where k is a temperature-dependent rate constant. Substitution of Eq. (2) into Eq. (1) and integration with the boundary condition $s(0) = s_0$ yields

$$s(z) = s_0 \exp\left(-\frac{keA}{v}z\right). \quad (3)$$

The energy-balance equation over the reactor volume, under isothermal and steady-state conditions, takes the form

$$Q_\infty - vs_0(-\Delta H_r)X_{\text{out}} = 0 \quad (4)$$

where Q_∞ is the thermal power transferred to the bath, and X_{out} the substrate conversion at the reactor outlet, equal to

$$X_{\text{out}} = 1 - \frac{s_{\text{out}}}{s_0}. \quad (5)$$

Combining Eqs. (3)–(5) gives

$$Q_\infty = vs_0(-\Delta H_r) \left[1 - \exp\left(-\frac{keV}{v}\right) \right]. \quad (6)$$

This equation allows estimation of k and ΔH_r from the experimental $Q_{\infty-s_0-T}$ data.

4.2. Estimation of the heat of reaction

The heat of reaction ($-\Delta H_r$) was estimated from experiments performed at 25 °C and higher enzyme concentration (series A in Table 1). Due to the low flow rate and high enzyme concentration, we assumed that the mean residence time of the liquid stream inside the reactor ($\tau_c = V/v$) was much higher than the characteristic reaction time ($\tau_r = 1/ke$), i.e. that the mixture leaving the reactor was at equilibrium.

Calculation of ΔG_r° for H_2O_2 decomposition from standard free energies of formation of products and reactants provides a value of -119 kJ mol^{-1} [23]. This corresponds to an equilibrium constant, at 25 °C, of 7.29×10^{20} , which indicates that the hydrogen peroxide conversion at the reactor outlet is practically unitary. Under these conditions the heat of reaction reduces to the ratio between the measured thermal power and the inlet substrate flow rate (see Eq. (4)). We obtained: $\Delta H_r = -87.55 \pm 0.72 \text{ kJ mol}^{-1}$. It should be noted that, when the hypothesis of unitary conversion holds, such estimate is no more affected by the flow model assumed for the reactor.

Table 2
Literature values for the heat of reaction

Reference	T (°C)	pH	$-\Delta H_r$ (kJ mol ⁻¹)
This study	25	7.4	87.55
[13]	25	7	88.88
[29]	25	7	83.67
[30]	25	7	86.75
[31]	37	8.2	88.99

As shown in Table 2, the heat of reaction determined in this work falls within the range of values reported in the literature, all of which were obtained by calorimetric techniques.

4.3. Estimation of kinetic parameters

Kinetic parameters were estimated from experiments labelled as series B–F in Table 1. They were performed at lower enzyme concentration ($1.8 \times 10^{-4} \text{ g l}^{-1}$) and with an inlet substrate concentration ranging from 2 to 10 mM. Due to the limited temperature range considered (10–30 °C), the heat of reaction was assumed to be temperature independent and equal to the value determined at 25 °C.

To describe the temperature dependence of the rate constant the following Arrhenius-type equation was considered:

$$k(T) = \exp\left[-\frac{E_a}{R}\left(\frac{1}{T} - \frac{1}{T^*}\right)\right] \quad (7)$$

where E_a is the apparent activation energy of reaction and T^* the temperature at which k is unitary. Estimation of E_a and T^* was carried out by minimisation of the following objective function:

$$\Phi(E_a, T^*) = \sum_{j=1}^N (Q_{\infty, j}^{\text{exp}} - Q_{\infty, j}^{\text{calc}})^2 \quad (8)$$

where N is the number of data points and the superscripts exp and calc denote experimental and calculated quantities, respectively.

Minimum search was performed by the Nelder–Mead simplex algorithm. It is a direct-search method which does not require gradient calculations or derivative information [24]. To find the global minimum we explored the parameter space by random generation of starting points. They were obtained as perturbations of the values resulting from a linear correlation

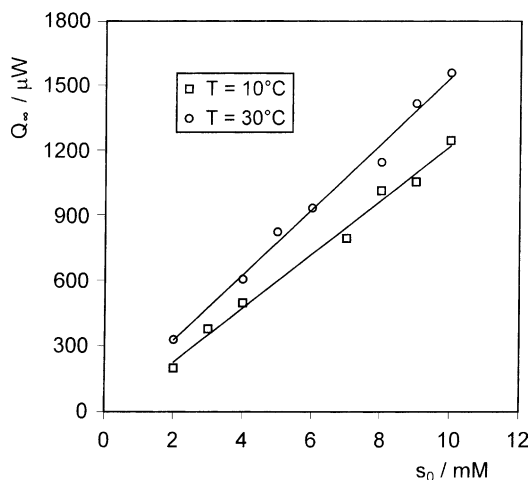


Fig. 3. Measured and calculated thermal powers (Q_∞) as a function of the inlet hydrogen peroxide concentration (s_0).

of $\ln k$ versus $1/T$. By this procedure we determined: $E_a = 11.0 \pm 1.2 \text{ kJ mol}^{-1}$, $T^* = 180 \pm 32 \text{ K}$. Some kinetic plots attesting the good agreement between experimental and calculated thermal powers are reported in Fig. 3. Similar results were obtained at the other temperatures investigated.

The activation energy estimated by us is close to the value of 8.8 kJ mol^{-1} found by Ghadermarzi and Moosavi-Movahedi [25] for bovine liver catalase, but is somewhat higher than those reported by Aebi [21] which range between 2.5 and 7.1 kJ mol^{-1} . In the latter reference, however, the biological source of the enzyme and its purity are not specified.

Knowing E_a and T^* allows calculation of k at any temperature. Fig. 4 shows the trend of the function $k(T)$. Data points were obtained from the experimental values of Q_∞ versus s_0 at each individual temperature. As can be seen, a temperature increase of 20°C (from 10 to 30°C) results in limited changes in k (from 14.5 to $19.91 \text{ g}^{-1} \text{ s}^{-1}$). This is clearly due to the low activation energy of reaction.

It is now possible to verify whether the assumption of equilibrium conditions for the mixture leaving the microcalorimeter, that was made on estimation of the heat of reaction, was correct. The ratio between τ_c and τ_r is:

$$\frac{\tau_c}{\tau_r} = \frac{Vke}{v} \quad (9)$$

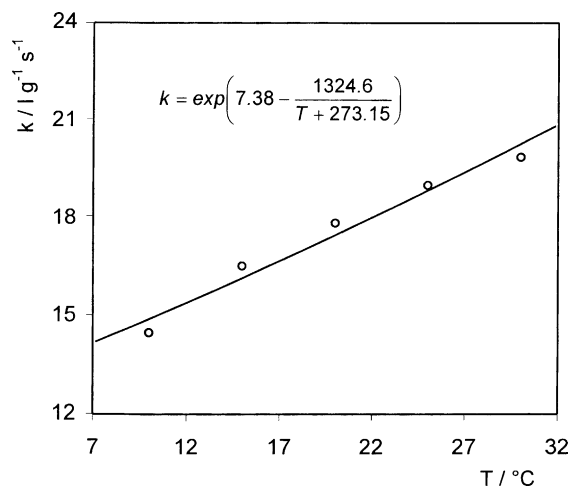


Fig. 4. Influence of temperature (T) on the apparent rate constant (k).

Substitution of the appropriate values ($V = 0.65 \text{ cm}^3$, $v = 0.23 \text{ cm}^3 \text{ min}^{-1}$, $k(25^\circ\text{C}) = 19.031 \text{ g}^{-1} \text{ s}^{-1}$, $e = 3.4 \times 10^{-2} - 6.8 \times 10^{-2} \text{ g l}^{-1}$) gives: $\tau_c/\tau_r \in [110, 220]$.

Since τ_c is two-orders of magnitude higher than τ_r , the hypothesis of equilibrium appears to be largely fulfilled.

4.4. Statistical analysis of results

The average percent error between calculated and measured thermal powers was 5.5%, with a standard

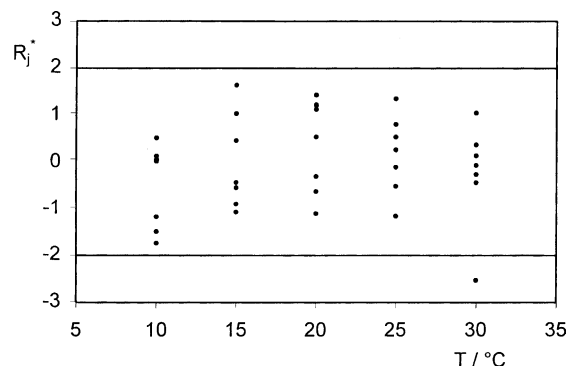


Fig. 5. Normalised model residuals (R_j^*) as a function of temperature (T). The horizontal lines ($R_j^* = \pm 2$) delimit the 95% confidence region.

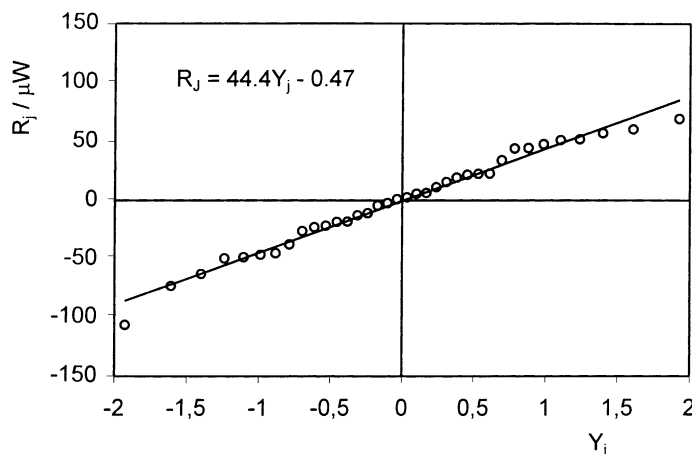


Fig. 6. Normal probability plot showing the trend of ordered residuals (R_j) against normal-order statistics medians (Y_j).

deviation of 5.8%. To assess the statistical significance of the results obtained we analysed the following model residuals:

$$R_j = Q_{\infty,j}^{\text{exp}} - Q_{\infty,j}^{\text{calc}} \quad (10)$$

which represent the differences between experimental values and model responses. In particular, in order to ensure that each data had the same statistical weight, we considered the following normalised residuals:

$$R_j^* = \frac{R_j}{\left[(1/(N-P)) \sum_{j=1}^N R_j^2 \right]^{0.5}} \quad (11)$$

where N is the number of data points ($N = 36$) and P the number of model parameters ($P = 2$). It can be shown that, if the error is normally distributed, 95% of the normalised residuals should be in the range (± 2) [26]. Residuals plotted against temperature gave the results shown in Fig. 5. As can be seen, residuals are uniformly scattered between -2 and $+2$, with just one outlier ($R_j^* = -2.53$) at the temperature of 30°C . In addition, no systematic temperature-related effect is observed.

As a further means of assessing the normality of the error distribution we made use of a normal probability plot [27]. It is obtained by plotting the ordered residuals, R_j , against the corresponding normal-order statistics medians, which are defined as

$$Y_j = F^{-1} \left(\frac{j}{N+1} \right) \quad (12)$$

where F is the standard normal cumulative distribution function. Data plotted in such a way should form an approximate straight line, with the intercept and slope representing, respectively, the location and scale parameters of the normal distribution. Departures from linearity are indicative of deviations from the assumed distribution. Furthermore, comparing the resulting correlation coefficient with a critical value, calculated for a given significance level and size of the data set, provides a formal test of normality [28].

Diagram plotted in Fig. 6 illustrates the results obtained. As apparent, a highly linear pattern is observed, with just limited deviations in the lower and upper extremes. The intercept and slope give estimates of -0.47 and $44.4 \mu\text{W}$, respectively, for the location and scale parameters.

At the 5% significance level, the critical value of the correlation coefficient for a set of 36 data points is 0.954 [28]. Since we obtained a value of $0.99 > 0.954$, the assumption that the data belong to a population with a normal distribution can not be rejected, i.e. the interpretation of microcalorimetric data by the model developed can be considered statistically correct.

5. Conclusions

The flow-mix arrangement can be effectively used to investigate enzymatic or, more generally, chemical kinetics by isothermal microcalorimetry. The

simplicity of use and the careful control of experimental conditions make it particularly attractive.

For the purpose of estimation of kinetic parameters, the calorimetric reaction unit can be schematised as a tubular reactor under plug-flow conditions. Of course, a more accurate description of the system under investigation would require modifying the assumed reacting-flow structure and removing the hypothesis of isothermal conditions for the reacting mixture.

As regards the kinetics of hydrogen peroxide decomposition, it should be emphasised that, at least up to a substrate concentration of 10 mM, the reaction rate can be considered to be of first-order with respect to both the substrate and the enzyme. In addition, no form of enzyme deactivation by the hydrogen peroxide seems to occur. Both considerations are validated by the good agreement between calculated and measured thermal powers, and by the statistical significance of the results obtained.

References

- [1] G. Buckton, *Thermochim. Acta* 248 (1995) 117.
- [2] V. Stefuca, P. Gemeiner, *Adv. Biochem. Eng. Biotechnol.* 64 (1999) 69.
- [3] A.E. Beezer, *Thermochim. Acta* 349 (2000) 1.
- [4] B. Schroll Harsted, E. Sonnich-Thomsen, *J. Chem. Thermodyn.* 6 (1974) 549.
- [5] M.M. Markovic, S.K. Milonjic, *Thermochim. Acta* 257 (1995) 111.
- [6] T. Friese, P. Ulbig, S. Schulz, K. Wagner, *J. Chem. Eng. Data* 44 (1999) 701.
- [7] M.M. Markovic, S.K. Milonjic, *Thermochim. Acta* 351 (2000) 153.
- [8] H. Aki, M. Goto, M. Yamamoto, *Thermochim. Acta* 251 (1995) 379.
- [9] E. Siimer, M. Kurvits, *Thermochim. Acta* 140 (1989) 161.
- [10] W. Riebesehl, E. Tomlinson, *J. Chem. Soc., Faraday Trans.* 79 (1983) 311.
- [11] M. Kurvits, E. Siimer, *Thermochim. Acta* 103 (1986) 297.
- [12] M. Beran, V. Paulicek, *J. Therm. Anal.* 38 (1992) 1979.
- [13] Y. Liang, Y. Wu, D. Li, C. Wang, Y. Liu, S. Qu, G. Zou, *Thermochim. Acta* 307 (1997) 149.
- [14] H. Sies, *Exp. Physiol.* 82 (1997) 291.
- [15] K. Stein, J.U. Hain, *Mikrochim. Acta* 118 (1995) 93.
- [16] L. Campanella, R. Roversi, M.P. Sammartino, M. Tomassetti, *J. Pharm. Biomed. Anal.* 18 (1998) 105.
- [17] L. Tarhan, *Process Biochem.* 30 (1995) 632.
- [18] F. Cioci, R. Lavecchia, P. Mazzocchi, *Chem. Eng. Sci.* 54 (1999) 3217.
- [19] G.R. Schonbaum, B. Chance, Catalase, in: P.D. Boyer (Ed.), *The Enzymes*, Academic Press, New York, 1976.
- [20] A. Deisseroth, A.L. Dounce, *Physiol. Rev.* 50 (1970) 319.
- [21] H.E. Aebi, Catalase, in: H.U. Bergmeyer (Ed.), *Methods of Enzymatic Analysis*, Verlag Chem., Weinheim, 1983.
- [22] B. Jiang, Y. Zhang, *Eur. Polym. J.* 29 (1993) 1251.
- [23] P.E. Liley, R.C. Reid, E. Buck, Physical and chemical data, in: R.H. Perry, D.W. Green (Eds.), *Perry's Chemical Engineers' Handbook*, McGraw-Hill, New York, 1984.
- [24] J.A. Nelder, R.A. Mead, *Comput. J.* 7 (1965) 308.
- [25] M. Ghadermarzi, A.A. Moosavi-Movahedi, *Ital. J. Biochem.* 46 (1997) 197.
- [26] H. Himmelblau, *Process Analysis by Statistical Methods*, Wiley, New York, 1970.
- [27] J. Chambers, W. Cleveland, B. Kleiner, P. Tukey, *Graphical Methods for Data Analysis*, Wadsworth, New York, 1983.
- [28] J.J. Filliben, *Technometrics* 17 (1975) 111.
- [29] Y. Liang, C.X. Wang, D.Q. Wu, Z.H. Song, S.S. Qu, G.L. Zou, *Huaxue Xuebao* 16 (1995) 924.
- [30] Y. Liang, C.X. Wang, Y.W. Liu, S.S. Qu, G.L. Zou, *Huaxue Xuebao* 58 (2000) 308.
- [31] W. Zhiyong, W. Cunxin, Q. Songsheng, *Thermochim. Acta* 360 (2000) 141.